Electronic properties of the semiconductor $RuIn_3$



2007 J. Phys.: Condens. Matter 19 232202

(http://iopscience.iop.org/0953-8984/19/23/232202)

IOP FTC

IOP PUBLISHING JOURNAL OF PHYSICS: CONDENSED MATTER

J. Phys.: Condens. Matter **19** (2007) 232202 (10pp) doi:10.1088/0953-8984/19/23/232202

**FAST TRACK COMMUNICATION**

# Electronic properties of the semiconductor $RuIn_3$

**D Bogdanov[1], K Winzer[1], I A Nekrasov[2] and T Pruschke[3]**

[1] Physikalisches Institut, Georg-August-Universität Göttingen, D-37077 Göttingen, Germany
[2] Institute of Electrophysics, Russian Academy of Sciences, 620016, Ekaterinburg, Russia
[3] Institut für Theoretische Physik, Georg-August-Universität Göttingen, D-37077 Göttingen, Germany

E-mail: kwinzer1@gwdg.de

Received 21 March 2007, in final form 18 April 2007
Published 17 May 2007
Online at stacks.iop.org/JPhysCM/19/232202

**Abstract**

Temperature-dependent measurements of the resistivity of $RuIn_3$ single crystals show a semiconducting behaviour, in contrast to previously published results (Roof *et al* 1986 *Powder Diffr.* **1** 20; Pöttgen 1995 *J. Alloys Compounds* **226** 59). In the high-temperature range the semiconducting gap was measured to be 0.4–0.5 eV. We observe an anisotropy of the resistivity along [110] and [001] orientations of the tetragonal single crystals. At low temperatures two activation energies of impurities were estimated to 1 and 10 meV. The temperature dependence of the specific heat and the band structure calculations also show a semiconducting behaviour of $RuIn_3$.

(Some figures in this article are in colour only in the electronic version)

## 1. Introduction

Intermetallic compounds formed by elemental metals with good conductivity are usually metallic conductors as well. A decade ago, Pöttgen [2], in a study of the crystal structure and physical properties of $RuIn_3$, reported on the metallic conductivity of this compound. However, for the isostructural compounds $FeGa_3$ and $RuGa_3$ electrical resistivity measurements revealed a semiconducting behaviour [3]. Since isostructural gallides and indides of the same group of transition elements have the same number of conduction electrons, the same type of conduction mechanism should be expected. All these compounds crystallize in the tetragonal $FeGa_3$ structure (space group $P4_2/mnm$) and should show anisotropic electrical properties.

The measurements on $RuIn_3$ [2] were performed on polycrystalline material obtained by solid-state reactions in sealed tantalum tubes, while the measurements on $FeGa_3$ and $RuGa_3$ [3] were performed on small unorientated single crystals grown from a Ga flux. In this article we report on anisotropic transport properties and on caloric properties on $RuIn_3$ single crystals, which confirm the semiconducting nature of this compound. The experimental results were strongly supported by local density approximation (LDA) band structure calculations, which

  

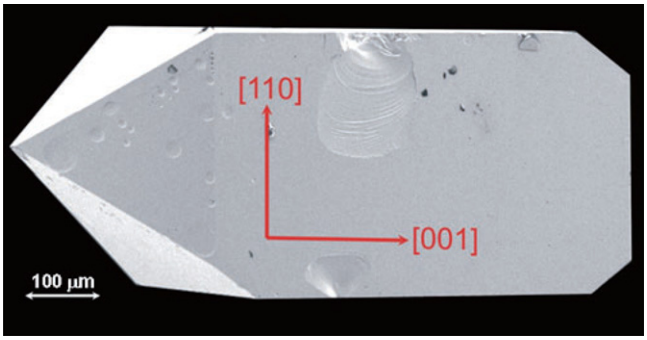


**Figure 1.** Scanning electron microscope picture of a well shaped $RuIn_3$ single crystal with {110} and {111} faces.

give an indirect band gap of 0.41 eV. Furthermore, the band structure calculations provide a qualitative explanation of the observed transport anisotropy.

## 2. Experimental details

Single crystals of $RuIn_3$ were grown using the flux method [4] with indium as reactant and as flux medium. An ingot of ruthenium ($\widetilde{=}$0.4 g) was placed at the bottom of a small $Al_2O_3$ crucible which was subsequently filled with liquid indium. The mass ratio of Ru to In used was about 1:20. The crucibles were wrapped in Zr foil and placed in a vertical tube furnace under flowing Ar at atmospheric pressure. Afterwards the furnace was heated to 1150 °C and cooled at a rate of 4 °C $h^{-1}$ to 600 °C, and below this temperature at a faster rate to 20 °C. The crystals were removed from the solidified In by heating the crucibles to 200 °C and decanting the liquid indium excess. The single crystals were then etched in dilute HCl to remove the residual In from their surfaces. Well-shaped silvery-grey crystals with sizes of up to 5 mm and masses of about 250 mg were typically obtained. The crystals consist of parallelepipeds with {110} faces and two pyramidal apices with {111} faces (see figure 1). The different faces of the single crystals were characterized by x-ray diffraction and the orientations were controlled by Laue diffraction. The stoichiometry of the crystals determined by energy-dispersive x-ray (SDX) analysis gives a composition of 25 ± 0.2 at.% Ru and 75 ± 0.45 at.% In.

To measure the anisotropy of the resistivity the Montgomery geometry [5] was chosen (see the inset in figure 2). The crystals were cut by spark erosion into cubes with edge lengths of 1.5 mm and supplied with four metallic contacts at the corners of the cubes. In addition, measurements of the Hall coefficient were performed on thin platelets of the same crystals. The measurements of the resistivity were done between 0.06 and 400 K with a standard lock-in technique. The measurements of the Hall coefficient and specific heat were performed between 2 and 300 K using a Quantum Design physical property measurement system (PPMS).

## 3. Results

The temperature dependence of the resistivity obtained by the Montgomery method on a single crystal of $RuIn_3$ is shown in figure 2. The resistivity ratio $\rho[110]/\rho[001] = 2.3$ at $T = 400$ K shows the anisotropy of the tetragonal crystals. The resistivity increases with decreasing temperature in the range from 400 to 270 K. In this temperature range the conductivity $\sigma(T)$ can simply be fitted by the equation $\sigma(T) = \sigma_0 \exp(-E_G/2k_BT)$ for the intrinsic conductivity of a semiconductor with an energy gap $E_G$. From the plot of $\ln(\sigma/\sigma_0)$ versus inverse temperature

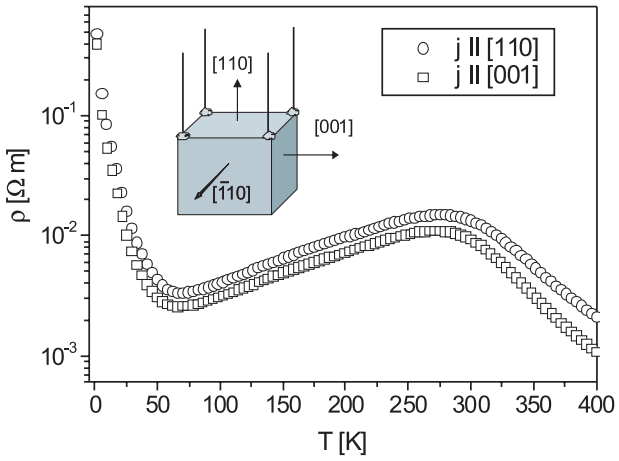


**Figure 2.** Temperature dependence of the resistivity of $RuIn_3$ for different crystallographic directions obtained by the Montgomery method. The inset shows a single crystal with contacts in Montgomery geometry.

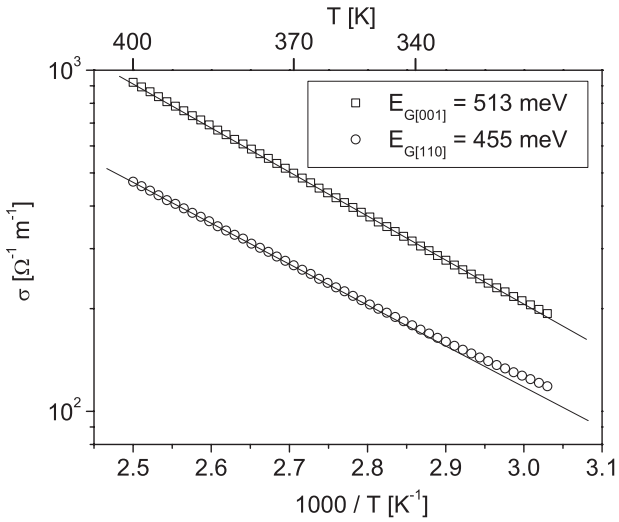


**Figure 3.** Conductivity as a function of inverse temperature for different directions in the temperature range of the intrinsic conductivity.

shown in figure 3 the gap energy of $RuIn_3$ can be estimated to be $E_{G[110]} = 0.455$ eV and $E_{G[001]} = 0.513$ eV, respectively.

In the temperature region between 270 and 120 K the Hall coefficient of all measured samples is more or less constant, and therefore the carrier concentrations were assumed to be constant. In this case the temperature dependence of the conductivity is caused by the temperature dependence of the mobility. If the scattering of the carriers is dominated by acoustic phonons a $T^{-3/2}$ dependence should be observed. Figure 4 shows the conductivities $\sigma(T)$ for both crystal orientations in a double-logarithmic plot together with a $T^{-3/2}$ straight line, which demonstrates that in the range 120 K $\leqslant T \leqslant$ 250 K the scattering is dominated by acoustic phonons.

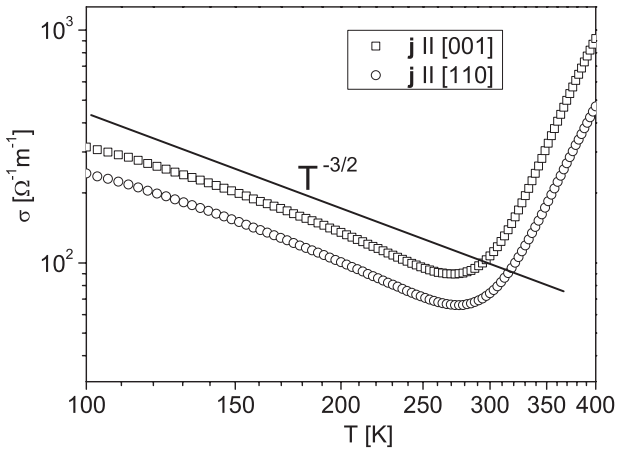


**Figure 4.** Conductivity of $RuIn_3$ versus temperature for both crystal orientations in a double-logarithmic plot together with a $T^{-3/2}$-dependence.

Below 120 K the Hall coefficient $R_H$ of the $RuIn_3$ single crystals is negative and increases with decreasing temperature. In this temperature range the conductivity diminishes caused by the freezeout of the extrinsic electrons and holes. Due to the different binding energies of the extrinsic carriers and the temperature dependence of the corresponding mobilities the temperature dependence of $R_H(T)$ is rather complex. In a two-band model with electrons and holes the Hall coefficient is given by

$$R_H(T) = \frac{1}{e} \times \frac{n_h \mu_h^2 - n_e \mu_e^2}{(n_h \mu_h + n_e \mu_e)^2} \tag{1}$$

with the concentrations $n_h$, $n_e$ and the mobilities $\mu_h$, $\mu_e$ of the holes and the electrons. From the measured conductivity $\sigma(T)$ and the Hall coefficient $R_H(T)$ the product

$$R_H(T) \times \sigma^2(T) = e \times (n_h \mu_h^2 - n_e \mu_e^2) \tag{2}$$

can be obtained, whose temperature dependence is easier to interpret. In figure 5 the product $R_H(T)\sigma^2(T)$ is given as a function of temperature. At low temperatures ($T < 20$ K) the value of $|R_H(T)\sigma^2(T)|$ is very small since most of the carriers are frozen at their impurity sites. $|R_H(T)\sigma^2(T)|$ steeply increases above 50 K, reaching a maximum at about 90 K. Since the sign of $R_H(T)\sigma^2(T)$ is negative, the increase is caused by the thermal activation of electrons from donors with a small activation energy $E_D$. Above 90 K $|R_H(T)\sigma^2(T)|$ decreases strongly, reaching $R_H(T)\sigma^2(T) = 0$ at about 150 K. The decrease of $|R_H(T)\sigma^2(T)|$ in the range $90\ \text{K} \leqslant T \leqslant 150$ K will be produced by the thermal activation of holes from acceptors with a larger activation energy $E_A$. It should be noted that $|R_H(T)\sigma^2(T)|$ is comparably small in the whole temperature range $150\ \text{K} \leqslant T \leqslant 300$ K. This could be a hint to the fact that both kinds of carrier originate from the same type of structural defect. The activation energies $E_D$ and $E_A$ can be obtained from the plot of $\ln(\sigma/\sigma_0)$ versus inverse temperature $T^{-1}$ in the temperature range $5\ \text{K} \leqslant T \leqslant 50$ K, which is given in figure 6. Typical values obtained for the activation energies on different single crystals are $E_D = 1.0$–$1.5$ meV for the donors and $E_A = 10$ meV for the acceptors. In the temperature range $T > 320$ K the quantity $R_H(T)\sigma^2(T)$ becomes negative again. In this regime intrinsic conductivity dominates and $n_h = n_e = n_i$. From $R_H\sigma^2 = e n_i(\mu_h^2 - \mu_e^2) < 0$ it follows that $\mu_e > \mu_h$, which in turn implies that $m_e^* < m_h^*$. The interpretation of this observation will be given in connection with band structure calculations.

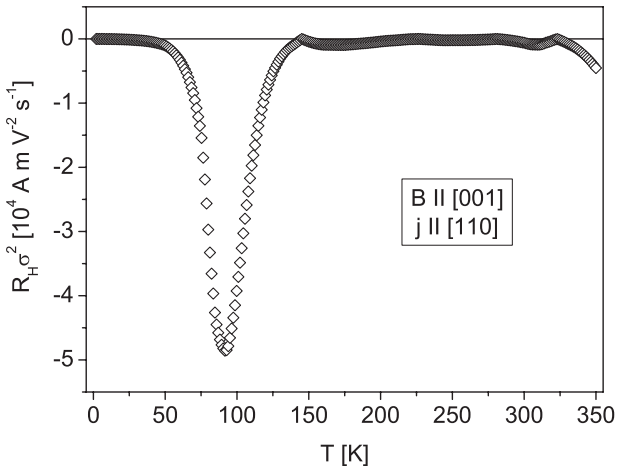


**Figure 5.** The product $R_{\mathrm{H}}(T)\sigma^2(T)$ as a function of temperature for the magnetic field $\mathbf{B} \parallel [001]$ and the current density $\mathbf{j} \parallel [110]$.

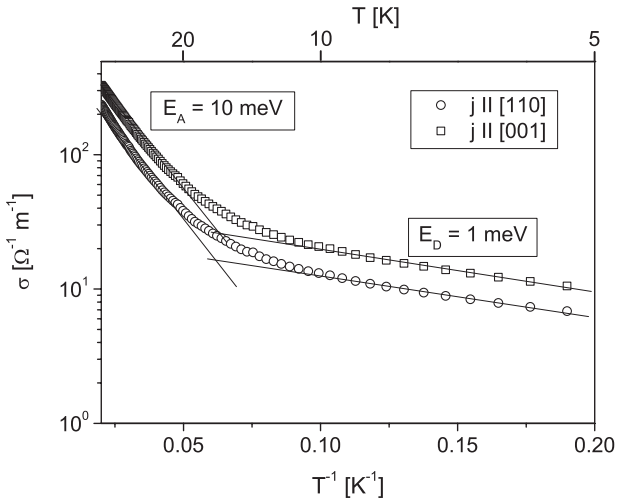


**Figure 6.** Conductivity as a function of inverse temperature for different crystal orientations in the temperature range $5\ \mathrm{K} \leqslant T \leqslant 50\ \mathrm{K}$.

The specific heat of $RuIn_3$, measured on a single crystal with a mass of $m \cong 25$ mg, is given in figure 7. $C(T)$ shows the typical temperature dependence of a semiconductor or an insulator in the temperature range $2\ \mathrm{K} \leqslant T \leqslant 300\ \mathrm{K}$ with a value of 100 J $\mathrm{mol}^{-1}$ $\mathrm{K}^{-1}$ at 300 K. The inset of figure 7 shows the low-temperature data ($2\ \mathrm{K} \leqslant T \leqslant 4\ \mathrm{K}$) in a $C/T$ versus $T^2$ plot. The extrapolation to $T = 0$ K goes through the origin, and indicates that the contribution of the carriers is very small. This fact corroborates the semiconducting behaviour of our transport measurements. The value of the slope is $A = 4.5 \times 10^{-4}$ J $\mathrm{mol}^{-1}$ $\mathrm{K}^{-4}$. From this result the Debye temperature $\Theta_{\mathrm{D}} = \left(\frac{12\pi^4 N k_{\mathrm{B}}}{5A}\right)^{1/3}$ of $RuIn_3$ can be calculated to be $\Theta_{\mathrm{D}} = 258$ K.

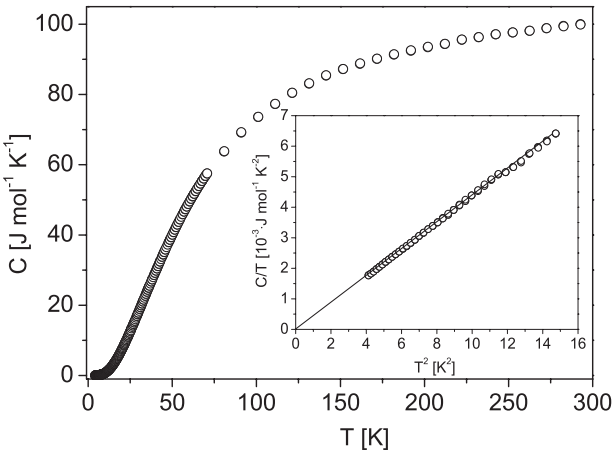


**Figure 7.** Specific heat of $RuIn_3$ in the temperature range 2 K $\leqslant T \leqslant$ 300 K. Inset: plot of $C/T$ versus $T^2$ in the low-temperature range 2 K $\leqslant T \leqslant$ 4 K.

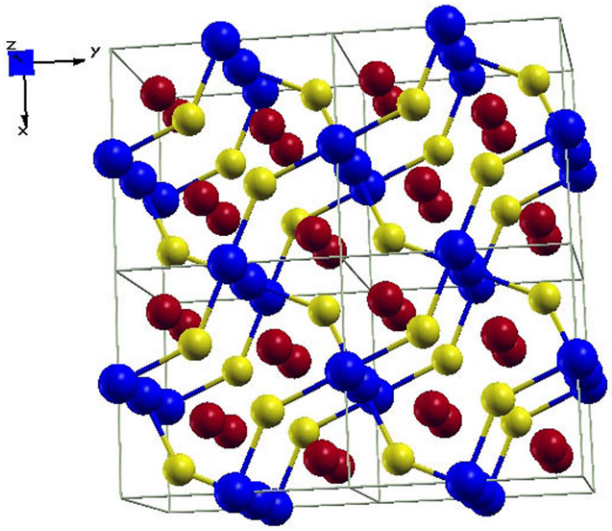


**Figure 8.** Crystal structure of $RuIn_3$. Red—In1 sites, blue—In2 sites, yellow—Ru sites.

## 4. Band structure calculation

State-of-the-art electronic structure calculations from first principles are based on density functional theory (DFT) within the local density approximation (LDA). To calculate the electronic structure of $RuIn_3$, the TB-LMTO-ASA package v. 47 (tight binding, linear muffin-tin orbitals, atomic sphere approximation) [6] was used with experimentally obtained values of the lattice constants ($a = b = 7.003$ Å, $c = 7.247$ Å, tetragonal space group $P4_2/mnm$ no. 136 [2]). The Ru sites occupy 4f Wyckoff positions ($x = 0.3451, y = 0.3451, z = 0$) and there exist two crystallographically inequivalent In sites at positions 4c for In1 ($x = 0, y = 0.5, z = 0$) and 8j for In2 ($x = 0.155\,47, y = 0.155\,47, z = 0.262\,24$). The crystal structure is presented in figure 8. Atomic spheres radii were chosen to be $R(\mathrm{Ru}) = 2.88$ au,

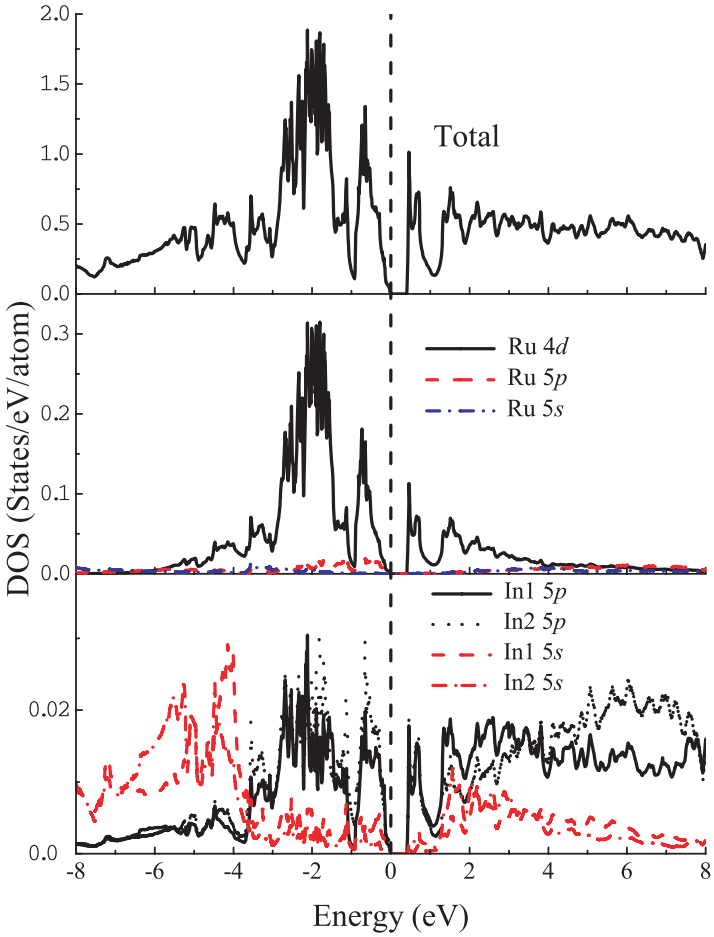


**Figure 9.** LDA calculated densities of states for $RuIn_3$. The upper panel shows the total DOS. The middle panel displays Ru 4d (full line), Ru 5p (dashed line) and Ru 5s (dotted line) states. The lower panel contains In1 5p (full line), In2 5p (long dashed line), In1 5s (dotted line) and In2 5s (dashed line) states. The Fermi level corresponds to zero.

$R(\mathrm{In1}) = 2.92$ au and $R(\mathrm{In2}) = 2.97$ au. The orbital basis consists of 5s, 5p, 4d muffin-tin orbitals for Ru and 5s, 5p for In1 and In2 sites. To fill the space of the unit cell several empty (without nuclei charge) atomic spheres were introduced. The calculations were performed with 405 irreducible **k**-points ($16 \times 16 \times 16$ spacing) in the first Brillouin zone.

In figure 9 we present the densities of states (DOSs) obtained within the LMTO method. The upper panel displays the total DOS with an energy gap of 0.41 eV. As is well known, DFT/LDA for semiconductors typically underestimates the band gap value by 15–30% (see for example [7]). On the other hand, TB-LMTO-ASA LDA calculations sometimes can in fact overestimate it a little bit due to the dependence of the gap on the choice of atomic radii. To provide a benchmark for $RuIn_3$, we in addition performed linearised augmented plane-wave (LAPW) calculations of the bandstructure. The value of the gap obtained within LAPW is 0.31 eV, which is smaller than both the experimental one and the one obtained with the LMTO method, as expected. More importantly, however, the qualitative results otherwise remain the same, in particular that

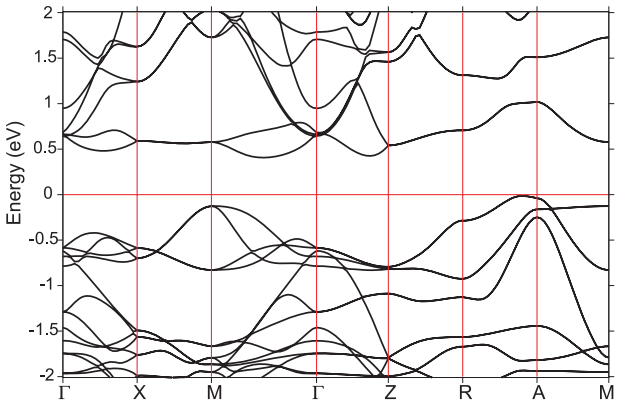


**Figure 10.** Band structure of $RuIn_3$ in the vicinity of the Fermi level calculated within standard DFT/LDA. The Fermi level corresponds to zero.

$RuIn_3$ is indeed a semiconductor and that the properties of the top of the valence band and bottom of the conduction band allow one to understand the experimentally observed anisotropy.

The individual contributions of Ru 5s, 5p and 4d states and the 5s, 5p states of both In sites to the total DOS are shown in the middle and lower panels of figure 9, respectively. By comparing the total and partial DOSs, one can identify several evident features. The energy range below $-4.5$ eV is dominated by In1(2) 5s states. In the energy interval $-4.5 \ldots 2$ eV one observes that the 5p states of In1 and In2 hybridize relatively strongly with Ru 4d states. Finally, above 2 eV there are predominantly In 5p states (see lower panel, figure 9).

The observed anisotropy of transport properties with different resistivities along the $ab$ and $c$ directions is quite generally consistent with the simple tetragonal crystal structure of the compound. In order to qualitatively explain why the $ab$ resistivity is larger than the one along $c$ we first note that the properties of hole transport will be determined by the top of the valence band located at **k**-point $(0.48, 0.48, 0.48)$ of the RA high-symmetry direction (see figure 10), because the energy gap is much larger than the experimental temperature and there are no other bands below this one within the interval of energies corresponding to the experimental temperature.

From the LDA band structure analyses one can conclude that the orbitals contributing to the top of the valence band along the RA high-symmetry direction in figure 10 can be separated into those lying in the $XY$-plane and those along the $Z$-axis. The former are superpositions of In2 $5p_x$, $5p_y$ and Ru $4d_{xz}$, $4d_{yz}$ orbitals, the latter obtained from In1 $5p_z$ and again Ru $4d_{xz}$, $4d_{yz}$ orbitals, and a small In2 $5p_z$ contribution[4]. There is also an In1 5s contribution to the top of the valence band which is anisotropic. Contributions of other symmetries are negligible.

The strongest orbital overlap is obtained for nearest neighbours. In the $XY$-plane these nearest neighbours are In2–Ru and Ru–Ru; In1 sites do not have nearest neighbours in the $XY$-plane. Along the $Z$-axis the nearest neighbours are Ru–In1 and In1–In2. Together with the previous classification of the orbitals contributing to the top of the valence band we can have In2–Ru pd$\pi$ hybridization (In2 $5p_z$ and Ru $4d_{xz}$ and $4d_{yz}$) and Ru–Ru dd$\delta$ hybridization (Ru $4d_{xz}$–$4d_{xz}$, Ru $4d_{yz}$–$4d_{yz}$) [8] in the $XY$-plane. These two types of hybridization are known to be quite weak [9]. Along the $Z$-axis the possible hybridizations are Ru–In1 sd$\sigma$ (Ru $4d_{xz}$,$4d_{yz}$

[4] Since $RuIn_3$ crystallizes in a tetragonal structure without distortions, there is no need to introduce a local coordinate system for each particular atom to properly resolve the orbitals with respect to their magnetic quantum number.

and In1 5s), In1–In2 sp$\sigma$ (In1 5s and In2 5p$_x$,5p$_y$,5p$_z$) and pp$\sigma$ (In1 5p$_z$ and In2 5p$_z$), which in principle are stronger [9] than the ones found for the $XY$-plane, thus qualitatively explaining the better conductivity along the $Z$-axis.

A similar argument can be applied to the electron transport dominated at low temperatures by the bottom of the conduction band in the middle of the ΓM direction.

Since the angles between bonds are not ideal in $RuIn_3$ (90° or 180°), there will of course be other types of hybridization. Furthermore, next-nearest-neighbour hoppings will contribute as well. All these effects will further reduce the anisotropy and lead to three-dimensional behaviour despite the layered structure of $RuIn_3$. Given all these partially compensating effects a final quantitative answer on the size of the anisotropy thus surely requires more detailed numerical investigations.

The band structure of $RuIn_3$ given in figure 10 shows a maximum of the valence band along RA in the Brillouin zone near A. The calculated effective hole mass is $m_h \approx 1.2m_0$. The minimum of the conduction band is formed by a flat band along ΓM with a large effective electron mass $m_{e1} \approx 2.6m_0$. Therefore in the intrinsic regime the quantity $R_H \times \sigma^2$ should be positive, in contrast to the observed high-temperature behaviour in figure 5. However, the band structure shows a second minimum of the conduction band along ΓZ near Z with a substantial smaller effective mass of $m_{e2} \approx 1.1m_0$. The energy difference between the two conduction band minima is only 20 meV, which is smaller as the thermal energy $k_BT$ at $T \geqslant 300$ K. Hence, the small effective electron mass $m_{e2}$ of the conduction band minimum near Z with the implication $\mu_{e2} > \mu_h$ is responsible for the negative sign of $R_H\sigma^2$ observed by the experiments in the intrinsic range.

## 5. Summary

Measurements of the resistivity and of the Hall coefficient of $RuIn_3$ single crystals identify this compound as a semiconductor with a gap energy of $E_G = 0.46$–$0.51$ eV, in contrast to previously published results, which report on metallic conductivity. The calculated band structure based on the density functional theory gives a similar value of $E_G = 0.41$ eV.

The experimentally observed slight anisotropy of the resistivity $\rho[110] > \rho[001]$ can qualitatively be explained by a theoretical symmetry analyses which predict a better conductivity along the $c$-axis of the tetragonal compound. The negative sign of the Hall coefficient in the intrinsic region can also be explained by the calculated conduction band structure with two energetically nearly equivalent minima but with very different effective electron masses.

In the extrinsic range at low temperatures a small activation energy for electrons from donors of $E_D = 1.0$–$1.5$ meV and a larger activation energy for holes from acceptors of $E_A = 10$ meV were determined from the transport measurements. Both kinds of extrinsic carrier seem to originate from the same type of structural defect, since $R_H\sigma^2$ is nearly zero in a large temperature range 150 K $< T <$ 320 K. The low-temperature data of the specific heat show a negligible contribution of charge carriers and corroborate the semiconducting nature of $RuIn_3$.

## Acknowledgements

IN thanks Postnikov for many helpful discussions. This work was supported in part by RFBR grants 05-02-16301 (IN), 05-02-17244 (IN), 06-02-90537 (IN), by the joint UrO-SO project (IN), and programmes of the Presidium of the Russian Academy of Sciences (RAS) ‘Quantum macrophysics’ and of the Division of Physical Sciences of the RAS ‘Strongly

correlated electrons in semiconductors, metals, superconductors and magnetic materials' and by the Deutsche Forschungsgemeinschaft through the collaborative research grant SFB 602 (TP, IN). IN acknowledges support from the Dynasty Foundation and International Center for Fundamental Physics in Moscow programme for young scientists and also from the grant of President of Russian Federation for young PhD MK-2242.2007.02, and thanks the Faculty of Physics of the Georg-August University of Göttingen for its hospitality.

## References

[1] Roof R B, Fisk Z and Smith D L 1986 *Powder Diffr.* **1** 20
[2] Pöttgen R 1995 *J. Alloys Compounds* **226** 59
[3] Häussermann U, Boström M, Viklund P, Rapp Ö and Björnängen T 2002 *J. Solid State Chem.* **165** 94
[4] See for instance Canfield P C and Fisk Z 1992 *Phil. Mag.* B **70** 1117 and references therein
[5] Montgomery H C 1971 *J. Appl. Phys.* **42** 2971
[6] Andersen O K, Jepsen O and Glötzel D 1985 *Highlights of Condensed-Matter Theory* ed F Bassani *et al* (Amsterdam: North-Holland)
Andersen O K and Jepsen O 1984 *Phys. Rev. Lett.* **53** 2571
[7] van Schilfgaarde M, Kotani T and Faleev S 2006 *Phys. Rev. Lett.* **96** 226402
[8] Slater J C and Koster G F 1954 *Phys. Rev.* **94** 1498
[9] Andersen O K, Klose W and Nohl H 1978 *Phys. Rev.* B **17** 1209